

Output Adaptive Control of a Skid Steering Autonomous Vehicle

1st Ruben Fuentes-Alvarez
UMI LAFMIA 3175 CNRS
CINVESTAV-IPN
Mexico City, Mexico
jose.fuentes@cinvestav.mx

2nd Isaac Chairez
Dept. of Bioprocesses
UPIBI-IPN
Mexico City, Mexico
jchairezo@ipn.mx

3rd Kim Adams
Faculty of Rehabilitation Medicine
University of Alberta
Edmonton, Canada
kdadams@ualberta.ca

4th Sergio Salazar
UMI LAFMIA 3175 CNRS
CINVESTAV-IPN
Mexico City, Mexico
sergio.salazar.cruz@gmail.com

5th Ricardo Lopez
UMI LAFMIA 3175 CNRS
CINVESTAV-IPN
Mexico City, Mexico
rricardooolopez@gmail.com

Abstract—This work presents the design as well as the evaluation of an output adaptive controller which must induce the stabilization of the tracking error for a class of skid steered autonomous vehicle (SSAV). The control design includes a nonlinear transformation (diffeomorphism) using a simplified SSAV mathematical model. This diffeomorphism justifies the transformation of the control problem in the original coordinates to a suitable chain of integrator system (third-order). In this study, the available measurements are the position and orientation of the SSAV. The aforementioned condition, encourages the implementation of a modified super twisting algorithm (STA) which is applied as a recursive differentiator which may estimate the velocity and acceleration of the SSAV efficiently. Based on the estimated states, an adaptive controller provides the asymptotic stability of the tracking trajectories for the SSAV. Numerical evaluation comparing the proposed adaptive controller with a state feedback controller confirmed the design of the suggested control structure.

Index Terms—Skid steering autonomous vehicle, super twisting, adaptive control

I. INTRODUCTION

An increasing interest in the developing mobile robotics has been observed in recent years [1]. The quantity of commercial wheeled mobile robot platforms available on the market is growing rapidly, presenting more constructive, but complex structures than the ones usually considered and for which modeling and control are still a relevant field of study [2]. Skid steering autonomous vehicles (SSAV) are commonly used to achieve different indoor and outdoor tasks due to its all-terrain capabilities [3]. The exclusion of the steering aspect makes the four wheeled differentially driven (4WDD) mobile vehicles robust in mechanics terminology, but also easily manoeuvrable when considering the problem of accurate trajectory tracking. As a consequence, the modification of SSAV orientation produces lateral slippage in the point where the wheels touch the ground making the control approach slightly different from the common wheeled mobile robotic devices [4]. When SSAV follows a non-straight path, the wheels required skidding laterally and they must not move tangentially to the reference trajectories [5]. Also, following a circular trajectory may produce some instantaneous center of rotation (ICR) of the SSAV to displace away of the robot wheelbase, causing some kind of instability. Lateral

friction on the wheels produces skidding forces, which motivates a specific control law design which may consider the mathematical description of the SSAV dynamics [6]. This consideration represents a strong difference between SSAV and vehicles using active steering kinematics as a consideration to design the controller. The skidding forces developed by wheels lateral friction motivate the design of a control based on the mathematical description of a skid steered mobile robot dynamics [6], which has embraced the design of new controllers. In [4], [7], a trajectory tracking and regulation closed-loop controller based on the back-stepping method was implemented, motivated by the unknown ground interaction forces and the dynamic uncertainties presented in the model of an SSAV. This solution shows to be robust against dynamic non modelled disturbances with an exponential time of convergence. The classical linear quadratic regulating control design (LQR) with a feed-forward part that compensates the non-linearities of the dynamic-drive SSAV model was developed in [8] In that study, it was observed that this type of algorithms is able to overcome the effects of non-linearities when tracking a reference trajectory. The solution presented in [9] provides a state feedback control considering the application of super-twisting algorithm which may stabilize the tracking error of the SSAV using a step-by-step sliding mode time derivator. This algorithm served to estimate the first and second derivatives. A path following algorithm based on adaptive discontinuous posture control was designed in [10]. Hybrid control strategies proposed by [11] took advantage of the concept of extended transverse functions to improve the performance of the controllers when reaching admissible reference motions. In addition, robust sliding mode fuzzy logic control was implemented as a trajectory tracking algorithm by [12] using a sequence of way points, trying to improve the mechanical system performance in the presence of uncertainties and external disturbances with minimum reaching time, distance error and smooth control actions. This study provides the following main contributions: a) a step by step high order differentiator to reconstruct the unknown states of the transformed SSAV dynamics, b) an adaptive output feedback controller which uses the estimated states provided by the output differentiator

and c) the numerical evaluation of the proposed methodology. Notice that the designed output adaptive controller implementing the third order step-by-step differentiator is not exhibiting the overshoot effect (which is common in this type of controllers). This may appear as an additional main contribution to the SSAV field. Section II describes the problem of controlling the SSAV skidding while turning. Section III introduces the mathematical description of the SSAV following the results from [6]. This section presents the complete methodology to clarify the transformation of the mathematical model of a SSAV into a chain of integrator that let implement the proposed controller. Section IV presents the description of a suggested step-by-step time differentiator, which can obtain the consecutive derivatives implemented in the control structure. In Section V the output adaptive control strategy is developed, presenting the mathematical proof, as well as the transformations that makes it feasible. The numerical evaluations comparing the proposed output adaptive controller against a linear controller with constant gain are presented in Section VI. Finally, Section VII closes the study with some final remarks on the obtained results.

II. PROBLEM STATEMENT

Let consider the SSAV must exert a path trajectory tracking despite the lateral skidding produced when the SSAV turns. If the dynamics of the SSAV is defined by the states ζ and the reference trajectories are defined by ζ^* , then the problem is to design an output feedback controller such that

$$\limsup_{t \rightarrow \infty} \|\zeta(t) - \zeta^*(t)\| = 0 \quad (1)$$

In particular, in this study, the SSAV must track a circular trajectory defined as follows:

$$\zeta^* = \begin{bmatrix} r \cos(\theta_c t) \\ r \sin(\theta_c t) \end{bmatrix} \quad (2)$$

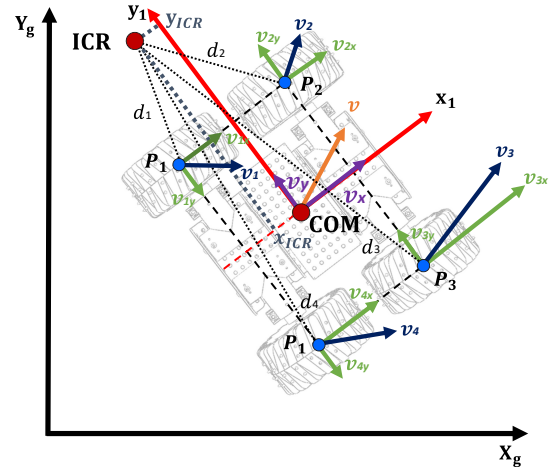
where r is the radius of the circle at constant speed θ_c at a time t . This available information z^* will be selected in such a way that the initial point D at a distance d_0 over the x -axis from the local inertial frame of the robot that corresponds to the non-holonomic constrain for the SSAV. The well suited problem statement requires that the SSAV exerts the circular movement following a tangential path to the reference trajectories.

III. MATHEMATICAL MODEL OF THE SSAV

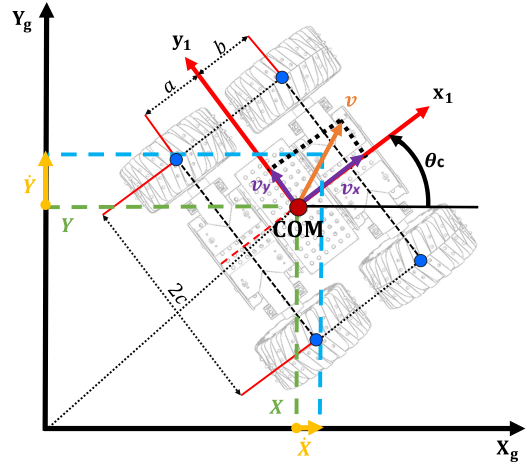
The dynamical model of the robot was inspired by the study given in [6]. The model is obtained under the following assumptions:

- Slow vehicle speed (for supporting the forward complete characteristic).
- The longitudinal wheel slippage is neglected.
- The tire lateral force is a function of the vertical load only.
- There is a neglecting of the suspension and tire deformations.
- No side-way movement (no sudden change of the frontal section of the mobile section).
- Both, SSAV mass and inertia are constant and known.

Assuming that no vertical movement of the SSAV is considered, the free-body scheme of the mobile section in x - y plane appears in Figure 1(a).



(a) Free body diagram of a SSAV.



(b) Forces and velocities acting on a SSAV.

Fig. 1. Caption place holder

The interaction forces between the surface and wheels are the lateral skidding and the friction forces. As wheels develop reactive forces $F_{jx} \left(\frac{dq}{dt} \right)$, they are restricted to the longitudinal resistance forces described by $R_{jx} \left(\frac{dq}{dt} \right)$, for $j = 1, \dots, 4$. It is assumed that wheel actuation is equal on each side, reducing longitudinal slip and causing lateral forces $F_{jy} \left(\frac{dq}{dt} \right)$ to act on the wheels because of the presence of the lateral skidding. This means that:

$$F_{1x} \left(\frac{dq}{dt} \right) = F_{4x} \left(\frac{dq}{dt} \right), \quad F_{2x} \left(\frac{dq}{dt} \right) = F_{3x} \left(\frac{dq}{dt} \right) \quad (3)$$

Notice that lateral skidding occurs when $\frac{d}{dt}y = 0$. Also, lateral skidding velocity $\frac{d}{dt}y_j$ and longitudinal velocity $\frac{d}{dt}x_j$ (for $j = 1, \dots, 4$) of each wheel are defined in (4):

$$\begin{aligned} \frac{d}{dt}y + c \frac{d}{dt}\theta_c &= \frac{d}{dt}y_2 = \frac{d}{dt}y_1 & (\text{front}) \\ \frac{d}{dt}y - d \frac{d}{dt}\theta_c &= \frac{d}{dt}y_4 = \frac{d}{dt}y_3 & (\text{rear}) \\ \frac{d}{dt}x + l \frac{d}{dt}\theta_c &= \frac{d}{dt}x_3 = \frac{d}{dt}x_2 & (\text{right}) \\ \frac{d}{dt}x - l \frac{d}{dt}\theta_c &= \frac{d}{dt}x_4 = \frac{d}{dt}x_1 & (\text{left}) \end{aligned} \quad (4)$$

The resistive moment $M_r \left(\frac{dq}{dt} \right)$ is generated by $R_{jx} \left(\frac{dq}{dt} \right)$ and $F_{jy} \left(\frac{dq}{dt} \right)$ forces as follows:

$$\begin{aligned} M_r \left(\frac{dq}{dt} \right) &= c \left(F_{1y} \left(\frac{dq}{dt} \right) + F_{2y} \left(\frac{dq}{dt} \right) \right) \\ -d \left(F_{3y} \left(\frac{dq}{dt} \right) + F_{4y} \left(\frac{dq}{dt} \right) \right) &+ l \left(R_{2x} \left(\frac{dq}{dt} \right) + R_{3x} \left(\frac{dq}{dt} \right) \right) \\ &- l \left(R_{1x} \left(\frac{dq}{dt} \right) + R_{4x} \left(\frac{dq}{dt} \right) \right) \end{aligned} \quad (5)$$

where the total longitudinal resistive forces and lateral forces are:

$$\begin{aligned} F_y \left(\frac{dq}{dt} \right) &= \frac{\mu mg}{c+d} \left(b \operatorname{sign} \left(\frac{dy_1}{dt} \right) + d \operatorname{sign} \left(\frac{dy_3}{dt} \right) \right) \\ R_x \left(\frac{dq}{dt} \right) &= \frac{f_r mg}{2} \left(\operatorname{sign} \left(\frac{dx_1}{dt} \right) + \operatorname{sign} \left(\frac{dx_2}{dt} \right) \right) \end{aligned} \quad (6)$$

assuming both the lateral friction coefficient μ and the coefficient of rolling resistance f_r constants independent from velocity. Also, the rotational movement is produced by the rotor effect forced by the motor and the rotational friction between the wheel and the shaft. The complications on the movement of the mobile section arise due to the presence of the lateral skidding [3], [5], [13].

The dynamics for the SSAV can be represented by the following nominal model:

$$M(q) \frac{d^2}{dt^2} q + Q \left(\frac{dq}{dt} \right) + f(q, t) = B(q) \tau \quad (7)$$

Here, $q^\top = [X \ Y \ \theta_c]$ defines the vector of state variables. The states X and Y describe the planar coordinates of the center of mass in the x -axis and y -axis respectively. The angle θ_c corresponds to the SSAV orientation as shown in Figure 1(b). The elements included in the model (7) are:

$$\begin{aligned} M &= \begin{bmatrix} m & 0 & 0 \\ 0 & m & 0 \\ 0 & 0 & I \end{bmatrix}, \quad B(q) = \frac{1}{R} \begin{bmatrix} \cos(\theta_c) & \cos(\theta_c) \\ \sin(\theta_c) & \sin(\theta_c) \\ -c & c \end{bmatrix}, \\ Q \left(\frac{dq}{dt} \right) &= \begin{bmatrix} F_{rx} \left(\frac{dq}{dt} \right) \\ F_{ry} \left(\frac{dq}{dt} \right) \\ M_r \left(\frac{dq}{dt} \right) \end{bmatrix} \end{aligned} \quad (8)$$

The functions $F_{Rx} \left(\frac{dq}{dt} \right)$ and $F_{Ry} \left(\frac{dq}{dt} \right)$ represent the forces affecting the wheels, which are generated by the lateral skidding as:

$$\begin{aligned} F_{Ry} \left(\frac{dq}{dt} \right) &= R_x \left(\frac{dq}{dt} \right) \sin(\theta_c) + F_y \left(\frac{dq}{dt} \right) \cos(\theta_c) \\ F_{Rx} \left(\frac{dq}{dt} \right) &= R_x \left(\frac{dq}{dt} \right) \cos(\theta_c) - F_y \left(\frac{dq}{dt} \right) \sin(\theta_c) \end{aligned} \quad (9)$$

The term $f(q, t)$ is the uncertain function representing the non-modeled section of the mathematical model (uncertainties) as well as the external perturbations. This work assumes that:

$$\|f(q, t)\|^2 \leq f^+, \quad f^+ \in \mathbb{R}^+ \quad (10)$$

Considering that the angular velocities are identical for the frontal and rear wheels (which are also assumed alike) at each side of the SSAV, the torques regulating its movement are:

$$\tau = \begin{bmatrix} \tau_L \\ \tau_R \end{bmatrix} = \begin{bmatrix} \tau_{L1} + \tau_{L2} \\ \tau_{R3} + \tau_{R4} \end{bmatrix} \quad (11)$$

where τ_L and τ_R are the torques for the left and right sides, respectively.

The free-body dynamics appears in equation (7). Such representation does not consider the non-holonomic restrictions inherent to the SSAV. Considering the non-inertial configuration of the mobile robot (Figure 1(b)), the x -axis projection of the center of rotation cannot be bigger than d . If such condition is violated, the vehicle skids along the y -axis, and the SSAV is not longer controllable. The proper vehicle movement requires the satisfaction of the following movement condition:

$$\left| -\frac{\frac{d}{dt}y}{\frac{d}{dt}\theta_c} \right| < d \quad (12)$$

Hence, the operative constraint [6] relating the y-linear and angular velocities, must be considered in the SSAV control design:

$$\frac{d}{dt}y + d_0 \frac{d}{dt}\theta_c = 0, \quad 0 < d_0 < d \quad (13)$$

where d_0 is the x -coordinate of the ICR, that is x_{ICR} . The non-holonomic restriction (13) is equivalent to (in generalized variables):

$$A(q) \frac{d}{dt}q = 0 \quad (14)$$

Here, $A(q) = [-\sin(\theta_c) \ \cos(\theta_c) \ d_0]$ and $\frac{d}{dt}q^\top = \left[\frac{d}{dt}X \ \frac{d}{dt}Y \ \frac{d}{dt}\theta_c \right]$. These non-holonomic constraints can be included in the dynamic model (7) using the Lagrange-multiplier technique:

$$\begin{aligned} M(q) \frac{d^2}{dt^2} q + Q \left(\frac{dq}{dt} \right) + f(q, t) \\ = B(q) \tau + A^\top(q) \lambda_i \end{aligned} \quad (15)$$

Here λ_i defines the vector of Lagrange multipliers associated to the restriction equations (14). Also, admissible generalized velocities $\frac{d}{dt}q$ can be represented as:

$$\frac{d}{dt}q = S(q)\eta \quad (16)$$

where $\eta \in \mathbb{R}^2$ refers to a pseudo-velocity and $S(q)$ is a 3×2 full range matrix, whose columns are in the null space of $A(q)$ as:

$$S \left(\frac{dq}{dt} \right) = \begin{bmatrix} \cos(\theta_c) & -\sin(\theta_c) \\ \sin(\theta_c) & \cos(\theta_c) \\ 0 & -d_0^{-1} \end{bmatrix} \quad (17)$$

Differentiating $\frac{d}{dt}q$ from equation (16) and eliminating λ from equation (15), the following dynamic system is obtained:

$$\begin{aligned} \frac{d}{dt}q = S\eta \\ \frac{d}{dt}\eta = \left(S^\top M S \right)^{-1} S^\top \left(E\tau - M \frac{d}{dt}S\eta - f(q, t) \right) \end{aligned} \quad (18)$$

Applying a nonlinear static state feedback law to (15), one may take the explicit control action τ from (18) as:

$$\tau = (S^\top E)^{-1} \left(S^\top M S u + S^\top M \frac{d}{dt}S\eta + S^\top c \right) \quad (19)$$

where $u = [u_1 \ u_2]^\top$ contains the new control variables, letting the reduced dynamic model becomes a pure second order kinematic model as follows:

$$\begin{aligned} \frac{d}{dt}q &= S\eta \\ \frac{d}{dt}\eta &= u \end{aligned} \quad (20)$$

This transformation is possible considering the following new set of variables:

$$\begin{aligned} \frac{d}{dt}X &= \cos(\theta_c)\eta_1 - \sin(\theta_c)\eta_2 \\ \frac{d}{dt}Y &= \sin(\theta_c)\eta_1 + \cos(\theta_c)\eta_2 \\ \frac{d}{dt}\theta_c &= -d_0^{-1}\eta_2 \\ \frac{d}{dt}\eta_1 &= u_1 \\ \frac{d}{dt}\eta_2 &= u_2 \end{aligned} \quad (21)$$

By choosing a particular output, the equation system presented in (21) can be linearized completely and decoupled by means of a dynamic state feedback. The position of a point D placed on the x -axis at a distance d_0 from the vehicle frame origin must be chosen as the selected linear output form:

$$\zeta = \begin{bmatrix} X + d_0 \cos(\theta_c) \\ Y + d_0 \sin(\theta_c) \end{bmatrix} \quad (22)$$

by adding a dynamic extension corresponding to the integration of the input u_1 :

$$\begin{aligned} u_1 &= \xi \\ \frac{d}{dt}\xi &= v_1 \\ u_2 &= v_2 \end{aligned} \quad (23)$$

where ξ is the controller state and v_1 and v_2 are the new control inputs. By decoupling the standard input-output, equation (22) is differentiated until the input v appears explicitly, obtaining:

$$\begin{aligned} \frac{d^3}{dt^3}\zeta &= \begin{bmatrix} \cos(\theta_c) & d_0^{-1}\eta_1 \sin(\theta_c) \\ \sin(\theta_c) & -d_0^{-1}\eta_1 \cos(\theta_c) \end{bmatrix} v \\ &+ \begin{bmatrix} d_0^{-2}\xi\eta_2 \sin(\theta_c) - 2d_0^{-2}\eta_1\eta_2^2 \cos(\theta_c) \\ -d_0^{-2}\xi\eta_2 \cos(\theta_c) - 2d_0^{-2}\eta_1\eta_2^2 \sin(\theta_c) \end{bmatrix} \\ &= \alpha(q, \eta)v + \beta(q, \eta) \end{aligned} \quad (24)$$

Since

$$\det[\alpha(q, \eta)] = -d_0^{-1}\eta_1 \quad (25)$$

the decoupling matrix α is non-singular if $\eta_1 \neq 0$. Whenever defined, the law control (under a certain relationship between X , Y and θ_c)

$$v = \alpha^{-1}(q, \eta)[r - \beta(\zeta, \eta)] \quad (26)$$

Here r is the trajectory jerk reference, yielding to

$$\frac{d^3}{dt^3}\zeta = r \quad (27)$$

The system (27) can be represented as

$$\begin{aligned} \frac{d}{dt}Z &= AZ + Br \\ Z &= \left[\zeta, \frac{d}{dt}\zeta, \frac{d^2}{dt^2}\zeta \right]^\top \end{aligned} \quad (28)$$

where A and B are controllable companion matrices of appropriate dimensions. Notice that the SSAV starts moving toward the corresponding trajectory by the application of an output adaptive controller τ . The goal of this controller is bringing the center of mass of the SSAV into the desired circular trajectory as the SSAV has the acceptable orientation (tangential movement).

The control design consider two steps: first the next section describes the application of a step by step differentiator. Once the no measurable states are estimated, the output feedback controller is developed.

IV. STATE ESTIMATION FOR THE SSAV

The realization of the output feedback controller requires the on-line measurements of ζ and its derivatives (at least to the second order) which are not available in principle. Instead of using the actual values of such derivatives, a robust high order differentiator based on a step-by-step super-twisting algorithm form, given by:

$$\begin{aligned} \frac{d}{dt}\hat{\zeta}_{1,j} &= \tilde{\zeta}_{2,j} + k_{11,j}\phi_{11}(e_{1,j}) \\ \frac{d}{dt}\tilde{\zeta}_{2,j} &= k_{12,j}\phi_{12}(e_{1,j}) \\ \frac{d}{dt}\hat{\zeta}_{2,j} &= E_{2,j} \left[\tilde{\zeta}_{3,j} + k_{21,j}\phi_{21}(e_{2,j}) \right] \\ \frac{d}{dt}\tilde{\zeta}_{3,j} &= E_{2,j} [k_{22,j}\phi_{22}(e_{2,j})] + v_{i,j} - \frac{d^3}{dt^3}\zeta_{i,j}^* \end{aligned} \quad (29)$$

with: $e_{i,j} = \tilde{\zeta}_{i,j} - \hat{\zeta}_{i,j}$. All the initial conditions for the observer (29) are zero. Notice here that $j = 1, 2$ represents the individual state included in ζ due to the this variable has two components.

The variables $\hat{\zeta}_{i,j}$ represent the corresponding estimated trajectories of $\zeta_{i,j}$. Consider that $\tilde{\zeta}_{1,j} = \zeta_{1,j}$ which is needed to complete the observer design. The indicator function $E_{i,j}(t)$ fulfills the following definition

$$E_{i,j}(t) = \begin{cases} 0 & t < T_{i,j}^* \\ 1 & t \geq T_{i,j}^* \end{cases} \quad (30)$$

The switching time $T_{i,j}^*$ is found as result of the fixed-time converge obtained for the observer [14]. The nonlinear functions $\phi_{1k}(e_k)$ and $\phi_{2k}(e_k)$ ($k = 1, 2$) were designed in agreement to the proposal given in [15]–[18]. Then, the following structures were considered for the observer design:

$$\phi_{1k}(e_i) = |e_i|^{1/2} \text{sign}(e_i), \quad \phi_{2k}(e_i) = \frac{1}{2} \text{sign}(e_i) \quad (31)$$

The details to adjust the gains $k_{11,j}$, $k_{12,j}$, $k_{21,j}$ and $k_{22,j}$ as well as the times when each section of the observer turns on $T_{i,j}$ appear in [14]. Notice that the observer (29) extends the dimensions of the state, which may introduce additional implementation complexity. However, the estimation quality of the derivatives of ζ_i produced by the suggested observer justifies such additional complexity, even if it should be implemented on-board for the SSAV. This step-by-step differentiator is not the unique possible solution to recover the states but it has a natural simplicity that may help to tune the gains easier than some other competitive options. Notice that high order sliding mode could offer interesting options but they gain tuning may take long periods and their embedded implementations could be energetic demanding.

V. ADAPTIVE CONTROL DESIGN FOR THE SSAV

Once the estimation of the state Z is ready and considering the forward complete characteristics of the SSAV dynamics, it is feasible to design the output feedback adaptive controller. Considering that the reference trajectory admits is at least twice differentiable, then exists a state variable representation given by $Z^* \in \mathbb{R}^6$ such that

$$\frac{d}{dt}Z^*(t) = AZ^* + Bh(Z^*(t), t) \quad (32)$$

Hence, the introduction of the tracking error $\Delta = Z - Z^*$ yields the following dynamics for the tracking error:

$$\frac{d}{dt}\Delta(t) = A\Delta(t) + B(r(t) - h(Z^*(t), t)) \quad (33)$$

Let propose the controller r as follows:

$$r(t) = h(Z^*(t), t) + K^\top(t)\Delta(t) \quad (34)$$

where K satisfies

$$\frac{d}{dt}K^\top(t) = -\alpha_Q\Delta(t)\Delta^\top(t)P + \tilde{K}^\top(t) \quad (35)$$

with $\alpha_Q = \lambda_{\min}P^{-1/2}QP^{-1/2}$ a positive scalar, and $P \in \mathbb{R}^{6 \times 6}$, $Q \in \mathbb{R}^{6 \times 6}$ positive definite matrices which regulates the time variation of the controller gain. This structure corresponds to the model reference adaptive control in the indirect form with the reference model given in (32). The deviation gain $\tilde{K}(t)$ satisfies $\tilde{K}(t) = K(t) - K^0$ with K^0 any matrix such that $A_K = A - BK^0$ is Hurwitz. The motivation to apply the adaptive control form is the necessity of compensating the potential perturbations affecting the SSAV as well as reducing the applied control energy during the tracking of the reference trajectory. The following lemma provides the main result of this study.

Lemma 1. *If the positive definite matrices Q and P are related by the following matrix inequality*

$$PA_K + A_K^\top P \leq -Q \quad (36)$$

then the origin is an exponential stable equilibrium point for the tracking error Δ with a rate of convergence given by α_Q .

Proof. Consider the following Lyapunov candidate function $V(\Delta, \tilde{K}) = \Delta^\top P \Delta + \text{tr} \left\{ \tilde{K}^\top \tilde{K} \right\}$. Then the time derivative of such candidate function is

$$\frac{d}{dt}V(t) = 2\Delta^\top(t)P\frac{d}{dt}\Delta(t) + 2\text{tr} \left\{ \tilde{K}^\top(t)\frac{d}{dt}\tilde{K}(t) \right\} \quad (37)$$

Taking the time derivative of Δ on (37) and noticing that $\frac{d}{dt}\tilde{K}(t) = \frac{d}{dt}K(t)$, one gets:

$$\begin{aligned} \frac{d}{dt}V(t) = & 2\Delta^\top(t)P(A\Delta(t) + B(r(t) - h(Z^*(t), t))) + \\ & 2\text{tr} \left\{ \tilde{K}^\top(t)\frac{d}{dt}K(t) \right\} \end{aligned} \quad (38)$$

The substitution of (34) in (38) provides

$$\begin{aligned} \frac{d}{dt}V(t) = & 2\Delta^\top(t)P(A\Delta(t) + B((K^*)^\top\Delta(t))) + \\ & 2\Delta(t)P\tilde{K}^\top(t)\Delta(t) + 2\text{tr} \left\{ \tilde{K}^\top(t)\frac{d}{dt}K(t) \right\} \end{aligned} \quad (39)$$

The algebraic manipulation of (40) yields

$$\begin{aligned} \frac{d}{dt}V(t) = & \Delta^\top(t)(PA_K + A_K^\top P) + \\ & 2\text{tr} \left\{ \tilde{K}^\top(t)\frac{d}{dt}K(t) + \tilde{K}^\top(t)\Delta(t)\Delta^\top(t)P \right\} \end{aligned} \quad (40)$$

Based on the adjustment law for the gain K , one gets

$$\frac{d}{dt}V(t) \leq -\Delta^\top(t)Q\Delta(t) - \text{tr} \left\{ \tilde{K}^\top \tilde{K} \right\} \quad (41)$$

Using the Raleigh's inequality, the following inclusion takes place

$$\frac{d}{dt}V(t) \leq -\alpha_Q V(t) \quad (42)$$

This inclusion finalizes the proof based on the application of the comparison principle and the direct integration of (42). \square

VI. NUMERICAL EVALUATIONS

Both the differentiator and the controller gains were computed using the theoretical results presented in the previous sections. The differentiator was simulated with the following gains:

$$k_{Obs} = \begin{bmatrix} 3 & 3 \\ 2 & 2 \end{bmatrix}, \quad K_{Ctrl} = \begin{bmatrix} -1 & -2.4142 & -2.4142 \end{bmatrix}$$

In Figure 2 the trajectories of the SSAV tracking a circular trajectory are shown, beginning at initial condition $(0,0)$. No overshoot was obtained by the output adaptive controller proposed in this paper. Also a comparison against a state feedback control was carried out, showing a smoother movement when converging to the trajectory.

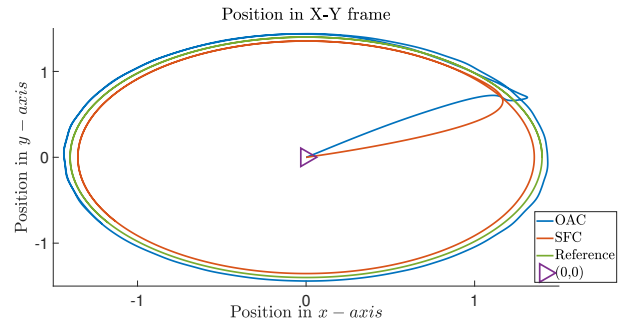
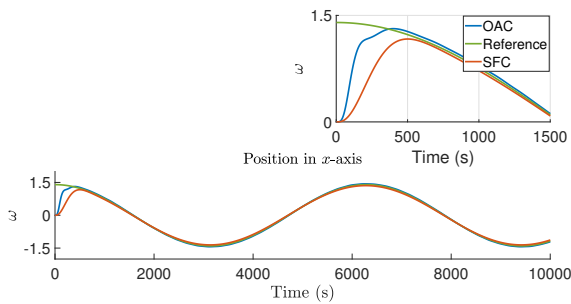


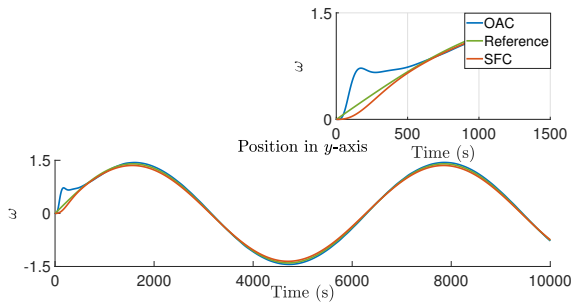
Fig. 2. SSMR trajectories in the xy plane. A second comparison is presented involving a state feedback controller and an output adaptive controller.

The convergence and smoothness of the trajectory approaching are depicted in Figure 3(a) for x -axis and Figure 3(b) for y -axis. In these figures, both the state feedback controller and the output adaptive controller are plotted, showing a smaller overshoot phenomenon in the output adaptive controller, without compromising the convergence time. The simulation time was established in Matlab-Simulink at 100 seconds using the Bogacki-Shampine (ode3) fixed-step solver.

Figure 4 shows the trajectory tracking error in logarithmic scale in each of the derivatives of the system. It can be observed that as the simulation converge to the desired trajectory, the error remains in 0.1 for the position, 0.15 for its primitive derivative and 0.2 for its second derivative respectively. The evolution of $\phi_{i,k}$ gains through time are presented in Figure 5, showing that the amount of energy



(a) Trajectories in the x-axis for the SSAV. Comparison between a state-feedback controller and an output adaptive control.



(b) Trajectories in the y-axis for the SSAV. Comparison between a state-feedback controller and an output adaptive control.

Fig. 3. Trajectories in the xy-frame.

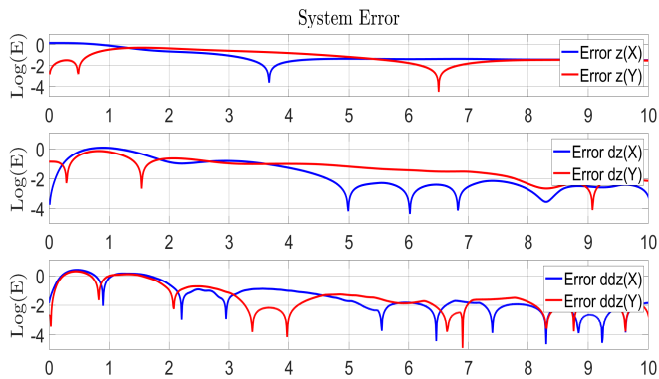


Fig. 4. System error.

consumed by the proposed step-by-step observer is nearly despicable. Also the chattering effect that is commonly presented by the STA can be observed as the signal converges to the origin.

VII. CONCLUSIONS

The design of the proposed output adaptive controller for trajectory tracking of an SSAV showed a similar time of convergence compared to the state-feedback controller in presence of modelling uncertainties. Also the effect of overshooting is observed to be reduced, generating a smoother convergence of the desired circular trajectory. Future works will describe the comparison of this scheme of control with different control algorithms, but also its implementation in an SSAV prototype.

REFERENCES

[1] R. S. Ortigoza, M. Marcelino-Aranda, G. S. Ortigoza, V. M. H. Guzman, M. A. Molina-Vilchis, G. Saldana-Gonzalez, J. C. Herrera-Lozada, and M. Olguin-Carbajal, "Wheeled mobile robots: A review,"

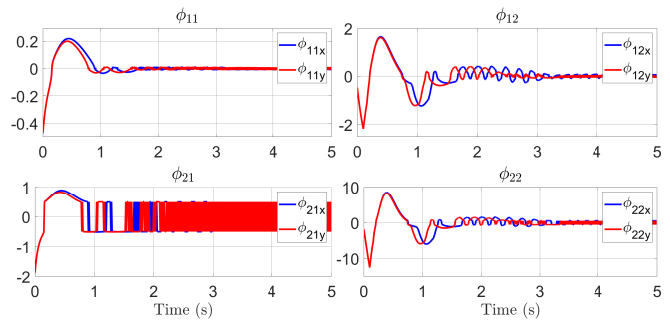


Fig. 5. Step-by-step differentiator gains evolution.

IEEE Latin America Transactions, vol. 10, no. 6, pp. 2209–2217, dec 2012.

- [2] G. Campion, G. Bastin, and B. Dandrea-Novet, "Structural properties and classification of kinematic and dynamic models of wheeled mobile robots," *IEEE Transactions on Robotics and Automation*, vol. 12, no. 1, pp. 47–62, 1996.
- [3] M. Trojnecki, *Dynamics Model of a Four-Wheeled Mobile Robot for Control Applications A Three-Case Study*, 01 2014, vol. 323, pp. 99–116.
- [4] K. Kozłowski and D. Pazderski, "Modeling and control of a 4-wheel skid-steering mobile robot," *International journal of applied mathematics and computer science*, vol. 14, pp. 477–496, 2004.
- [5] J. Yi, H. Wang, J. Zhang, D. Song, S. Jayasuriya, and J. Liu, "Kinematic modeling and analysis of skid-steered mobile robots with applications to low-cost inertial-measurement-unit-based motion estimation," *IEEE Transactions on Robotics*, vol. 25, no. 5, pp. 1087–1097, oct 2009.
- [6] L. Caracciolo, A. De Luca, and S. Iannitti, "Trajectory tracking control of a four-wheel differentially driven mobile robot," in *Proceedings 1999 IEEE International Conference on Robotics and Automation (Cat. No. 99CH36288C)*, vol. 4. IEEE, 1999, pp. 2632–2638.
- [7] D. Pazderski and K. Kozłowski, "Trajectory tracking control of skid-steering robot – experimental validation," *IFAC Proceedings Volumes*, vol. 41, no. 2, pp. 5377–5382, 2008.
- [8] O. Elshazly, A. Abo-Ismael, H. S. Abbas, and Z. Zyada, "Skid steering mobile robot modeling and control," jul 2014.
- [9] I. Salgado, D. Cruz-Ortiz, O. Camacho, and I. Chairez, "Output feedback control of a skid-steered mobile robot based on the super-twisting algorithm," *Control Engineering Practice*, vol. 58, pp. 193–203, jan 2017.
- [10] F. Ibrahim, A. A. Abouelsoud, A. M. R. F. Elbab, and T. Ogata, "Path following algorithm for skid-steering mobile robot based on adaptive discontinuous posture control," *Advanced Robotics*, vol. 33, no. 9, pp. 439–453, apr 2019.
- [11] D. Pazderski and K. Kozłowski, "Motion control of a skid-steering robot using transverse function approach-experimental evaluation," in *2015 10th International Workshop on Robot Motion and Control (RoMoCo)*. IEEE, 2015, pp. 72–77.
- [12] V. Nazari and M. Naraghi, "Sliding mode fuzzy control of a skid steer mobile robot for path following," dec 2008.
- [13] H. Wang, J. Zhang, J. Yi, D. Song, S. Jayasuriya, and J. Liu, "Modeling and motion stability analysis of skid-steered mobile robots," may 2009.
- [14] N. Martínez-Fonseca, I. Chairez, and A. Poznyak, "Uniform step-by-step observer for aerobic bioreactor based on super-twisting algorithm," *Bioprocess and Biosystems Engineering*, vol. 37, no. 12, pp. 2493–2503, jun 2014.
- [15] A. Chalanga, S. Kamal, L. M. Fridman, B. Bandyopadhyay, and J. A. Moreno, "Implementation of super-twisting control: Super-twisting and higher order sliding-mode observer-based approaches," *IEEE Transactions on Industrial Electronics*, vol. 63, no. 6, pp. 3677–3685, jun 2016.
- [16] T. Gonzalez, J. A. Moreno, and L. Fridman, "Variable gain super-twisting sliding mode control," *IEEE Transactions on Automatic Control*, vol. 57, no. 8, pp. 2100–2105, aug 2012.
- [17] A. Davila, J. A. Moreno, and L. Fridman, "Optimal lyapunov function selection for reaching time estimation of super twisting algorithm," dec 2009.
- [18] E. Cruz-Zavala, J. A. Moreno, and L. M. Fridman, "Uniform robust exact differentiator," *IEEE Transactions on Automatic Control*, vol. 56, no. 11, pp. 2727–2733, 2011.